

Simulation Optimization Of Vibration-Based Energy Harvesters For EV Application

Chandan Pandey.¹, Barun Pratiher²

1. Department of Mechanical Engineering, IIT, Jodhpur, Rajasthan, India.

2. Department of Mechanical Engineering, IIT, Jodhpur, Rajasthan, India.

Abstract

Vibration-based Piezoelectric Energy harvesters convert ambient vibration energy into an applicable electrical charge for wireless sensors, IoT applications, and charging the battery, which is most important to range improvement of the Electric Vehicle. This study analyses different beam configurations from Industrial machines, such as simple, Tapered, L-shape, and U-shape Cantilever configurations with Proof mass. Nonpiezoelectric to piezoelectric ratio is taken as more than unity and formulated linear dynamics equation of the entire structure for unimorph beam. The electromechanical Coupling behavior of such configuration with respect to important performance parameters is analytically evaluated and validated with COMSOL Multiphysics simulation. After analysis of the beam configuration, it is found that a U-shape unimorph Cantilever can generate a maximum power of 23.5 mW and a maximum Voltage of 22.4 V among all Configurations. Using this work, researchers can optimize and design performance energy harvesters for various industrial applications or the role of COMSOL multiphysics for energy harvesting.

Keywords: Energy Harvesting, Piezoelectric effect, COMSOL simulation, Electromechanical coupling.

Introduction

Ambient energy exists in various forms within our environment, including light, radio signals permeating the air, motion from wind or vibrations, and the flow of heat. These diverse energy sources can be harnessed through various methods. This micro-scale energy harvesting process involves utilizing transducers, which may consist of photovoltaic cells, thermal generators, or vibrational generators. While the energy levels available in the ambient environment are typically modest and incapable of meeting the power demands of a household, they prove sufficient for numerous applications. These applications encompass the realms of ambient intelligence, devices for monitoring conditions, implantable and wearable electronics, as well as wireless sensor networks, where the energy can effectively power small electronic devices [1]. The description pertains to the utilization of a wireless power node for energy harvesting or charging a battery system [2]. Several instances of applications involving vibration harvesting include kinetic watches, monitoring industrial motors, assessing the health of structures and bridges, operating light switches powered by kinetic energy, utilizing muscle-powered implants, and employing helicopter tracking nodes. These applications are further elaborated upon in the explanation [3]. Harvesters with electromagnetic convert kinetic energy into electricity after shifting a coil across the magnetic field of an immobile magnet, which results in the induction of voltage across the coil. While these electromagnetic generators can produce substantial output currents,

the voltage they generate tends to be quite low, usually less than 1 volt. The construction of macro-scale devices involves the use of large performance-based multi-turn coils or bulk magnets. However, due to the substantial magnetic components involved, electromagnetic harvesters tend to be weighty and sizable [4]. The discussion revolves around the extraction of sources of energy such as solar, and thermal, and the vibrations due to human walk. It focuses on specific parameter values. It's important to note that piezoelectric elements undergo physical deformation when exposed to an electric field and generate the charge under deformation. One notable aspect is that the energy density of piezoelectric transducers surpasses that of electrostatic and electromagnetic counterparts by a factor of three. This heightened energy density makes piezoelectric transduction particularly appealing to researchers [5]. Piezoelectric generators are constructed from dielectric materials that accumulate charge when subjected to stress. These generators offer the benefits of straightforward design and uncomplicated manufacturing. Furthermore, they are readily combined with silicon-made devices and can be further processed alongside microelectronic circuits on the same chip [6]. Stress or strain relation described for piezoelectric materials relationship in reference [7]. In this context, 'T' signifies the stress arising from the combination of electrical and mechanical influences, while ' σ ' denotes the stress solely caused by mechanical factors. A practical approach to creating models for piezoelectric elements, which facilitates the rapid development of system equations, involves representing both the electrical and mechanical

aspects of the piezoelectric system as circuit components. The electromechanical coupling with the transformer is studied in the model [8]. Analytical solutions in closed form for vibration energy harvesters subjected to base excitation are developed using the Euler-Bernoulli beam model. These solutions pertain to both unimorph and bimorph energy harvesters, considering both series and parallel connections [9]. The piezoelectric ceramic's elastic constant is subsequently employed, in combination with the moment of inertia, while also considering the variable Young's modulus of the central shim [10]. [11] The equations for a linear piezoelectric material have been derived in a matrix format. Additionally, analytical models for estimating power, solving Euler-Bernoulli equations of motion, examining mode shapes, and studying beam behavior under various boundary conditions are thoroughly explored [12,13,14]. Moreover, an electrical representation model is established for the beam with a tip mass, in which voltage depends on the thickness and electric displacement of PZT. This formulation incorporates the energy conservation equation and the electro-mechanical interaction of the beam, particularly in the bimorph section. Validation of this model is carried out using Ansys [15,16]. Hosseini et al.[17] investigated how the geometric shape of a bimorph piezoelectric cantilever impacts power generation efficiency. Utilized the Euler-Bernoulli beam theory to compute the natural frequency and then validated these calculations using ABAQUS. The voltage variations of a PVDF energy harvester has been analyzed through COMSOL simulation, considering parameters such as gap size, proof mass, and the Rayleigh damping coefficient.[18]. Chen et al.[19] described an innovative piezoelectric energy harvester employing a bi-stable curve design with an adjustable potential wall was discussed with the aim of enhancing the output voltage, either through analytical methods or COMSOL simulation. Based on the literature review conducted above, it is evident that vibration-based energy harvesters utilizing COMSOL Multiphysics are constrained when applied to various structural configurations. In response to this limitation, this study focuses on developing an analytical model and employing COMSOL simulations for a piezoelectric generator. The aim is to optimize the generator's geometric dimensions to maximize power output. In pursuit of this goal, we have derived equations of motion and electromechanical equations for different geometric shapes, including simple shapes, tapered shapes, L-shapes, and U-shapes for energy harvesting. The electrical power or voltage generated by these harvesters can be used to charge a battery, which, when designed at a macro scale, has the potential to enhance the range of an electric vehicle (EV). While the present study primarily selects micro-scale harvesters utilizing unimorph beams, the applications described in the introduction section could be extended to EV applications in the future.

Mathematical Modelling

Developing an analytical model for the harvesters serves two purposes: it not only aids in assessing the effective power output from a source of vibration but also elucidates relationships that provide valuable insights to enhance system performance. Furthermore, this model can be integrated into an optimization process to fine-tune geometric design parameters. With these objectives in focus, we embark on creating a mathematical model for the piezoelectric generator depicted in Figure 1.

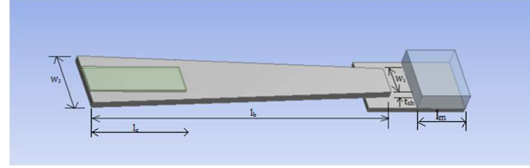


Figure 1. Tapered beam with unimorph harvesters.

We assume the configuration of an unimorph element that bends affixed as a cantilever beam, as illustrated in Figure 1. As is commonly observed in such elements that are bent, the material is oriented with polarization along the Z axis, and electrodes are affixed to the surfaces perpendicular to the Z axis. We further assume that the vibrational forces act exclusively along the Z axis. Under these established conditions, the piezoelectric material undergoes a one-dimensional state of stress along the X-axis. In this specific stress context, the piezoelectric equations are found in equations (1) and (2).

$$\{S\} = [s^E]\{T\} + [d^T]\{E\} \quad (1)$$

$$\{D\} = [d]\{T\} + [\epsilon^T]\{E\} \quad (2)$$

In this context, $\{S\}$ denotes the 6-dimension-based strain vector, $\{T\}$ represents stresses, $\{D\}$ stands for the 3-dimensional electric displacement, and $\{E\}$ signifies the electric field. $[s^E]$ is a (6×6) compliance matrix evaluated at a constant electric field, $[d]$ is a (3×6) matrix of piezoelectric strain components, and $[\epsilon^T]$ is a (3×3) dielectric constant matrix evaluated at a constant stress. Figure 2 depicts an equivalent circuit for the bender system shown in Figure 1. Within this circuit, the equivalent inductor, denoted as L_m , symbolizes the mass or inertia of the generator, while the equivalent resistor R_b , signifies mechanical damping. The equivalent capacitor, C_k , represents mechanical stiffness. σ_{in} represents an equivalent stress generator that models the stress generated due to input vibrations. The variable 'n' represents the equivalent turns ratio of the transformer, and C_b is the capacitance of the piezoelectric bender. V corresponds to the voltage across the piezoelectric device. On the mechanical side of the circuit, the variable 'across' corresponds to stress, σ (analogous to voltage), and the variable 'through' corresponds to strain rate, S (analogous to current). By utilizing this modeling approach, the mechanical side of the circuit is treated as an independent mechanical system, decoupled from other influences. Hence, the stress variable employed here is denoted as σ , rather than T , and the

relationship between stress and strain is expressed as $S = s\sigma$ (or $\sigma = cS$). The transformer, in this context, represents the piezoelectric coupling, similar to how transformers are characterized by a turns ratio that links voltage between two sides. In this particular scenario, stress on the mechanical side corresponds to voltage on the electrical side. Much like conventional electrical circuits, the system equations are derived through the application of Kirchhoff's voltage law (KVL) and Kirchhoff's current law (KCL). The summation of 'voltages' around the mechanical aspect of the circuit leads to the equation found in (3), while aggregating the currents at the point depicted in Figure 2 yields the equation presented in (3).

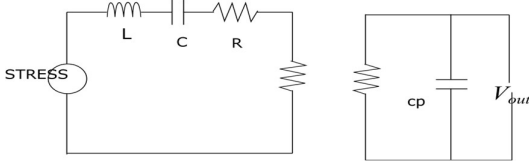


Figure 2. Circuit representation of the piezoelectric generator.

$$\sigma_{in} = L_m \ddot{S} + R_b \dot{S} + \frac{S}{C_k} + nV, \quad i = C_b \dot{V} \quad (3)$$

To convert these expressions into a practical system model, we must establish equivalent expressions for σ_{in} , L_m , R_b , C_k , n , and i . Given that the piezoelectric bender is a composite beam, we can compute the effective moment of inertia using the equation (4) provided below.

$$I(x) = \left[\frac{wt_c^3}{12} + wt_p b^2 \right] + \eta_s \left(\left(\frac{w_1 - w_2}{L} \right) x + w_2 \right) \frac{t_{sh}^3}{12} \quad (4)$$

The width of the piezoelectric material is denoted as 'w,' while 'w₁' and 'w₂' represent the widths of the beam. The parameter ' η_s ' signifies the ratio of the elastic constant of the central shim to that of the

Where,

$$B' = \left(l_b + l_e + \frac{l_m}{2} \right), \quad O' = \left(\left(\frac{w_1 - w_2}{L} \right) \left(\frac{t_c^3}{6} + 2t_p b^2 + \eta_s \frac{t_{sh}^3}{12} \right) \right), \quad N' = w_2 \left(\frac{t_c^3}{6} + 2t_p b^2 + \frac{\eta_s t_{sh}^3}{12} \right)$$

Remembering that $F_{in} = m\ddot{y}$, the expression for σ_{in} becomes

$$\sigma_{in} = k_1 m \ddot{y} \quad (9)$$

The stress across the 'inductive' element in Figure 2 is a result of the inertial force $F_m = m\ddot{z}$. The stress induced by inertial effects can then be written as

$$\sigma_m = k_1 m \ddot{z} \quad (10)$$

The equivalent inductance of this element, L_m , relates stress to the second time derivative of strain rather than displacement as in equation (10). In order

Where k_2 be defined as the relationship between z and S expressed as

piezoelectric material ($\eta_s = c_{sh}/c_p$, where ' c_p ' stands for the elastic constant of the piezoelectric material, and ' c_{sh} ' represents the elastic constant of the central shim). Subsequently, the elastic constant for the piezoelectric ceramic is used in conjunction with the effective moment of inertia as defined in equation (4). The variable ' η_s ' accommodates the different Young's modulus of the central shim in the moment of inertia. The equivalent input stress, σ_{in} , results from the input force, F_{in} , which arises directly from the input vibrations (\ddot{y}). As a consequence, σ_{in} can be expressed as $\sigma_{in} = k_1 F_{in}$, where ' k_1 ' represents a geometric constant that links the average stress in the piezoelectric material to the force exerted by the mass at the end of the beam. In order to derive an expression for k_1 , consider the expression for the average stress in the beam, σ , as shown in equation (5).

$$\sigma = \frac{1}{l_e} \int_0^{l_e} \frac{M(x)b}{I} dx \quad (5)$$

where $M(x)$ is the moment, and l_e is the length of the piezoelectric material. The expression for the moment is given by

$$M(x) = m(\ddot{y} + \ddot{z}) \left(l_b + l_e + \frac{1}{2} l_m - x \right) \quad (6)$$

The term $m(\ddot{y} + \ddot{z})$ is really a combination of input force, F_{in} , and inertial force, F_m . Substituting $F = F_{in} + F_m = m(\ddot{y} + \ddot{z})$ into equation (6), equation (6) into (5), and integrating yields the following expression:

$$\sigma = F \frac{b}{l_e} \left[\frac{B'}{O'} + \frac{N'}{O'^2} \right] \left[\ln \left(\frac{O' l_e + N'}{N'} \right) \right] - \frac{b}{O'} \quad (7)$$

The constant, k_1 , is then

$$k_1 = \frac{b}{l_e} \left[\frac{B'}{O'} + \frac{N'}{O'^2} \right] \left[\ln \left(\frac{O' l_e + N'}{N'} \right) \right] - \frac{b}{O'} \quad (8)$$

to derive the expression for L_m , an expression relating average strain, S , to vertical displacement, z , needs to be obtained. Consider the standard beam equation shown in equation (11).

$$\frac{d^2 z}{dx^2} = \frac{1}{c_p I} m(\ddot{y} + \ddot{z}) \left(l_b + l_e + \frac{1}{2} l_m - x \right) \quad (11)$$

Integrating to obtain an expression for the deflection term, z , and on substituting $\sigma = c_p S$ and $m(\ddot{y} + \ddot{z}) = F$ into equation (6) above, strain can be written as shown below.

$$z = S k_2 \quad (12)$$

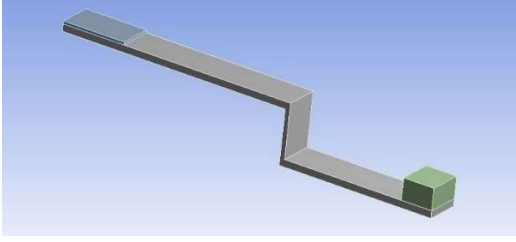
$$k_2 = k_1 \left[\left(\frac{B'}{O'^2} + \frac{N'}{O'^3} \right) \left((O'(l_b + l_e) + N') (\ln(O'(l_b + l_e) + N') - 1) \right) - \frac{N'}{O'^2} - \frac{l_b^2}{2O'} + 0.783(l_b + l_e) + 13.34 \right] \quad (13)$$

Once we have k_1 and k_2 , all the basic electrical calculations will be the same as in Roundy et al.[15]. The voltage (V) and power (P) formula when the excitation frequency matches the system frequency be

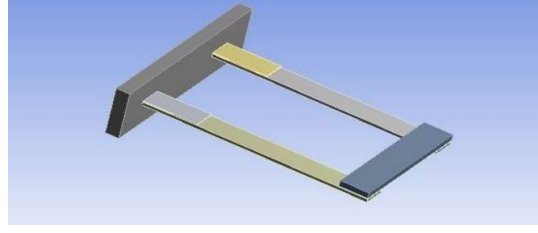
$$V = \frac{j\omega \frac{2c_p d_{31} t_c}{a\varepsilon} A_{in}}{j\omega \left(\omega^2 k_{31}^2 + \frac{2\zeta\omega}{RC_b} \right) - 2\zeta\omega^3 k_2}, P = \frac{1}{2\omega^2} \frac{C_b^2 \left(\frac{2c_p d_{31} t_c}{k_2 a\varepsilon} \right)^2 A_{in}^2}{(4\zeta^2 + k_{31}^4)(RC_b\omega)^2 + 4\zeta k_{31}^2 (RC_b\omega) + 4\zeta^2} \quad (19)$$

Using the same procedure explained above for the Tapered beam into L-shape and U-shape harvesters, we obtained the following terms for k_1 and k_2 .

L - Shape Configuration



U-shape Configuration



$$k_1 = \frac{b}{2I} [3l_b + l_m], k_2 = \frac{(19l_b^3 - 6l_m l_b^2 - \frac{3l_b l_m^2}{2})}{9b(l_m + 4l_b - l_e)}$$

$$k_1 = \frac{b(2l_b + l_m - l_e)}{I}, k_2 = \frac{l_b^2 (2l_b + \frac{3}{2}l_m)}{3b(2l_b + l_m - l_e)}$$

COMSOL Simulation

The COMSOL software was employed to analyze the piezoelectric energy harvester, aiming to anticipate how the harvester's geometries are linked to its output characteristics. The COMSOL software was used to construct a comprehensive model of the piezoelectric energy harvester. Additionally,

boundary conditions were imposed on the clamped end of the cantilever, ensuring zero displacement for all degrees of freedom at the nodes. Figure 3 displays the COMSOL model, highlighting various geometric shapes along with their respective meshing patterns, including simple, tapered, L-shape, and U-shape configurations of the piezoelectric energy harvester.

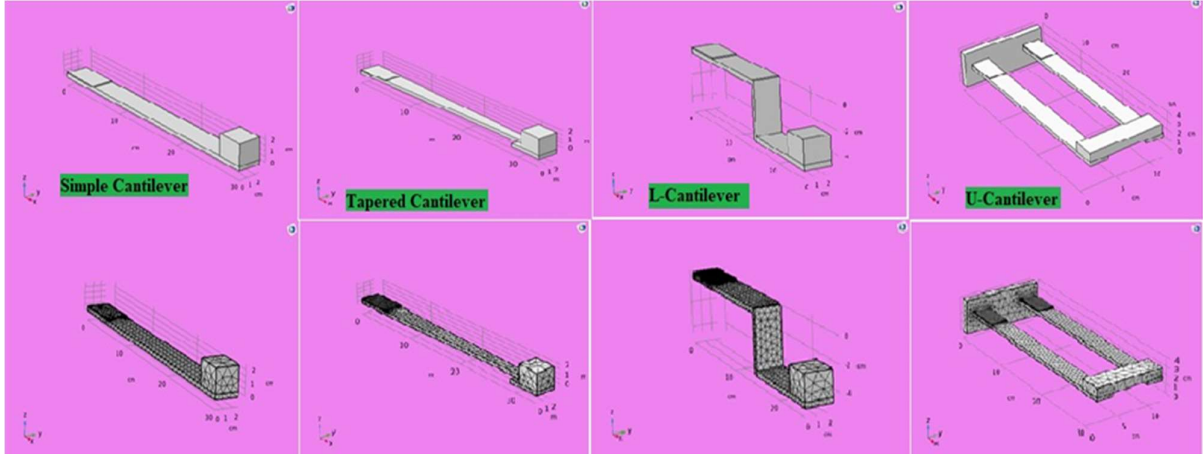


Figure 3. Energy harvesters with different geometric shape.

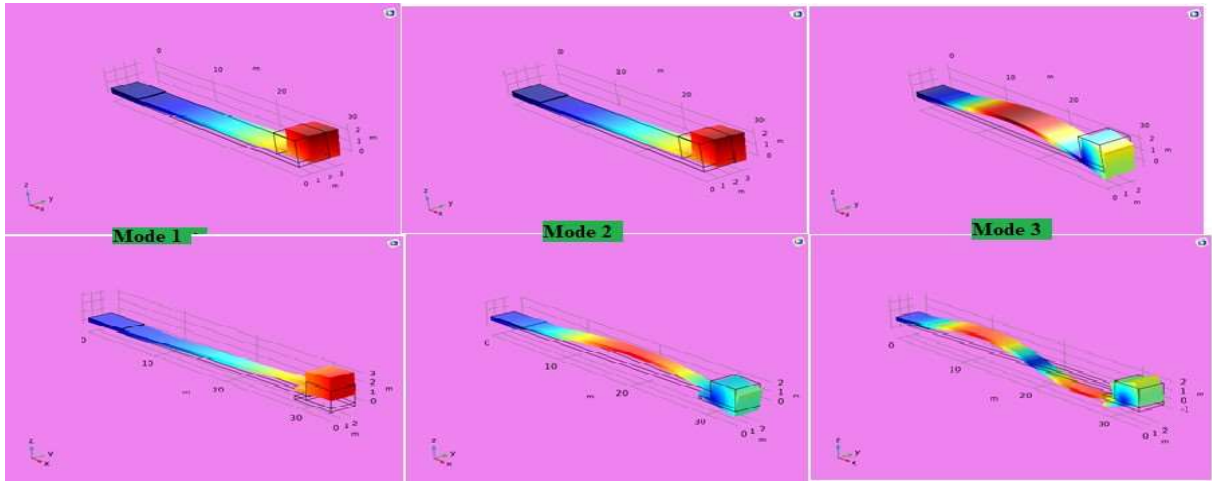


Figure 4. Mode shape for simple and tapered harvesters.

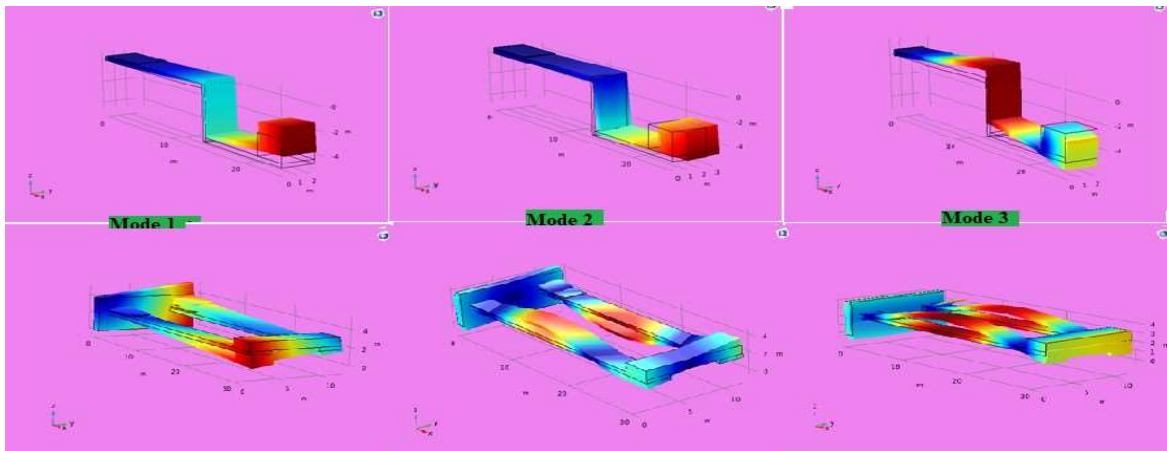


Figure 5. Mode shape for L-shape and U-shape harvesters.

Results and Discussion

The beam length L and width of all the shape is taken as 30 cm and 2.54 cm, respectively, but 1cm for the

Tapered end side for tapered harvesters and the Table 1 parameters are taken into analysis.

Table 1

t_{sh} (mm)	t_c (mm)	E_s (Gpa)	E_p (Gpa)	mass(gm)	d_{31} (m/V)	ϵ_{33} (F/m)
4	1	69	66	60	$180 e^{-12}$	$1800 \epsilon_0$

Table 2

Mode	Mode 1		Mode 2		Mode 3	
	Analytical	COMSOL	Analytical	COMSOL	Analytical	COMSOL
Simple Cantilever	43.074	42.75	230.05	230.95	323.31	321.75
Tapered Cantilever	41.226	34.686	246.14	243.22	302.01	307.43
L-shape	39.116	37.358	123.65	128.67	246.06	241.37
U-shape	34.48	29.68	201.12	199.24	433.66	431.13

To begin, a modal analysis is performed on the model established in COMSOL, as depicted in Figure 3. This analysis is carried out to identify the vibration modes and their associated resonance frequencies. For the simple cantilever energy harvester, the first three resonance frequencies are determined to be 43.074 Hz, 230.05 Hz, and 323.31 Hz, respectively. The magnitude of the resonance frequency for the tapered, L-shape, and U-shape

amplitude of 0.6 N in the form of a tip mass. Our observations reveal that, under a 10 k Ω load resistance and a 3g input acceleration, the simple cantilever generates approximately 4.2 mW of power and reaches a voltage of 8.4 V. The analytical and COMSOL-derived variations in voltage and power with respect to frequency are summarized in Table 3. Additionally, Figure 6 and Figure 7 illustrate how voltage and power vary across different beam configurations. Notably, it is apparent

Table 3

Configuration	Simple Cantilever		Tapered Cantilever		L-shape Cantilever		U-shape Cantilever	
	V	P (mW)	(V)	(mW)	Voltage	P (mW)	Voltage	P (mW)
Analytical	8.4	4.2	12.6	12.5	14.6	15.5	20.4	23
COMSOL	8.6	4.21	13.46	11.2	14.8	13.8	22.4	23.2
Relative Error	2.3 %	0.238%	6.825%	10.4 %	1.36%	10.96	9.80	0.869%

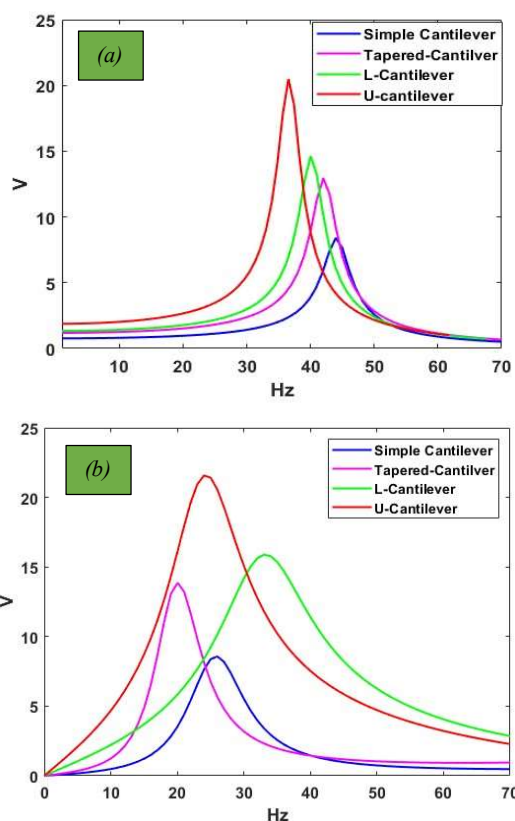


Figure 6. Voltage variation with frequency (a) Analytical (b) COMSOL

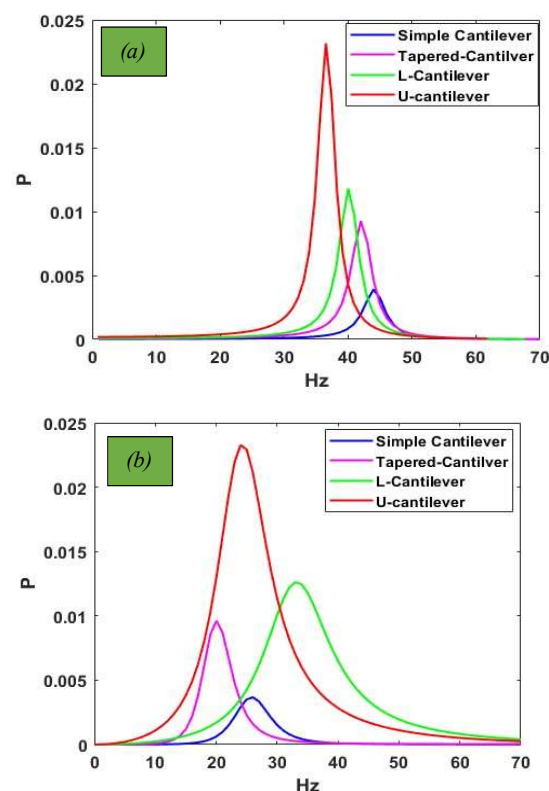


Figure 7. Power Variation with frequency (a) Analytical (b) Comsol

harvesters are presented in Table 2. In order to harness the maximum electrical power from piezoelectric elements attached to vibrating structures, it's essential to excite these structures at their first natural frequency, where they exhibit the most substantial deflections. In our investigation, the straightforward cantilever beam is stimulated at its initial natural frequency, denoted as $\omega_1 = 43.074$ Hz. The graphs in Figure 6 and Figure 7 depict how the output voltage and power fluctuate with changing frequencies. To verify these findings, we conducted a COMSOL simulation involving a configured beam subject to an external force with an

that the output power and voltage exhibit relatively minor discrepancies when comparing analytical results with those obtained through COMSOL Multiphysics.

Conclusion

As the size and power consumption of wireless electronic devices continue to decrease, the feasibility of powering such devices through ambient vibrations becomes increasingly promising. We conducted an analysis and developed models for a range of energy harvesting generators featuring piezoelectric unimorph membrane structures. These generators were able to produce a maximum power output of 23.5 mW when subjected to an acceleration

of 3g and connected to a load resistance of 10 k Ω . Our efforts included the creation of an analytical model for a simple cantilever piezoelectric generator, along with the proposal of an equivalent electromechanical circuit. The analytical results were successfully validated by comparing them with simulations conducted using COMSOL Multiphysics. We constructed and tested four different designs with resistive loads. Among these optimized designs, the U-shaped configuration proved to be the most efficient, delivering a maximum power output of 23.5mW and a maximum voltage of 22.4V, while keeping other parameters constant. This research provides valuable insights for researchers seeking to optimize energy harvester designs, particularly for potential applications in electric vehicles when scaled up to the macro level.

References

- [1] Roundy, Shad, Paul Kenneth Wright, and Jan M. Rabaey, "Energy scavenging for wireless sensor networks", *Norwell*, pp.45-47,2003.
- [2] Roundy and Shad,"Improving power output for vibration-based energy scavengers", *IEEE Pervasive computing*,pp.28-36, 2005.
- [3] White, N. M., Peter Glynne-Jones, and S. P. Beeby,"A novel thick-film piezoelectric micro-generator", *Smart Materials and Structures*,pp.850,2001.
- [4] Umeda, Mikio, Kentaro Nakamura, and Sadayuki Ueha, "Analysis of the transformation of mechanical impact energy to electric energy using piezoelectric vibrator", *Japanese Journal of Applied Physics*, pp.3267,1996.
- [5] Bayrashev, Andrey, William P. Robbins, and Babak Ziaie,"Low frequency wireless powering of microsystems using piezoelectric–magnetostrictive laminate composites", *Sensors and Actuators A: Physical* ,pp.244-249,2004.
- [6] Erturk, A and Inman, D. J,"A Distributed Parameter Electromechanical Model for Cantilevered Piezoelectric Energy Harvesters", *ASME. J. Vib. Acoust*, pp. 041002,2008.
- [7] Roundy, Shad, Paul K. Wright, and Kristofer SJ Pister, "Micro-electrostatic vibration-to-electricity converters",*ASME international mechanical engineering congress and exposition*,pp.487-496, 2002.
- [8] El-Hami, M., P. Glynne-Jones, N. M. White, M. Hill, Stephen Beeby, E. James, A. D. Brown, and J. N. Ross, "Design and fabrication of a new vibration-based electromechanical power generator",*Sensors and Actuators A: Physical*, pp.335-342,2001.
- [9] Erturk, Alper, and Daniel J. Inman. "An experimentally validated bimorph cantilever model for piezoelectric energy harvesting from base excitations",*Smart materials and structures*,pp.025009,2009.
- [10] Ottman, Geoffrey K., Heath F. Hofmann, and George A. Lesieutre,"Optimized piezoelectric energy harvesting circuit using step-down converter in discontinuous conduction mode", *IEEE Transactions on power electronics*,pp.696-703,2003.
- [11] Roundy, Shad, and Paul K. Wright, "A piezoelectric vibration based generator for wireless electronics", *Smart Materials and structures*,pp. 1131,2004.
- [12] Amirtharajah, Rajeevan, and Anantha P. Chandrakasan,"Self-powered signal processing using vibration-based power generation." *IEEE journal of solid-state circuits*, pp.687-695,1998.
- [13] Shu, Y. C., and I. C. Lien, "Analysis of power output for piezoelectric energy harvesting systems", *Smart materials and structures*,pp. 1499,2006.
- [14] Nechibvute, Action, Albert Chawanda, and Pearson Luhanga, "Piezoelectric energy harvesting devices: an alternative energy source for wireless sensors",*Smart Materials Research* pp.2012,2012.
- [15] Yan, Z., and L. Y. Jiang,"The vibrational and buckling behaviors of piezoelectric nanobeams with surface effects", *Nanotechnology*,pp.245703,2011.
- [16] Kundu, Sushanta, and Harshal B. Nemade, "Modeling and simulation of a piezoelectric vibration energy harvester",*Procedia Engineering*, pp.568-575,2016.
- [17] Hosseini, Rouhollah, Omid Zargar, and Mohsen Hamedi, "Improving power density of piezoelectric vibration-based energy scavengers", *Journal of Solid Mechanics*, pp. 98-109,2018.
- [18] Cepenas, Mindaugas, Bingzhong Peng, Darius Andriukaitis, Chandana Ravikumar, Vytautas Markevicius, Neringa Dubauskiene and Dangirutis Navikas,"Research of PVDF energy harvester cantilever parameters for experimental model realization", *Electronics*,pp. 2030,2020.
- [19] Chen, Xiaoyu, Xuhui Zhang, Luyang Chen, Yan Guo, and Fulin Zhu,"A curve-shaped beam bistable piezoelectric energy harvester with variable potential well: modeling and numerical simulation", *Micromachines*, pp. 995,2021.